IEEE Access
Multidisciplinary ⋮ Rapid Review ⋮ Open Access Journal

Received February 1, 2020, accepted February 20, 2020, date of publication February 24, 2020, date of current version March 4, 2020.

Digital Object Identifier 10.1109/ACCESS.2020.2976138

A Flexible Supraharmonic Group Method Based on Switching Frequency Identification

YINGXIN WANG[1], YONGHAI XU[1], (Member, IEEE), SHUN TAO[1], (Member, IEEE), ABUBAKAR SIDDIQUE[2], AND XU DONG[1]

[1]State Key Laboratory of Alternate Electrical Power System with Renewable Energy Sources, North China Electric Power University, Beijing 102206, China
[2]Department of Electrical Engineering, Khwaja Fareed University of Engineering and Information Technology (KFUEIT), Rahim Yar Khan 64200, Pakistan

Corresponding author: Shun Tao (tao_shun@sina.com)

This work was supported by the National Natural Science Foundation of China under Grant 51777066.

ABSTRACT The extensive use of power electronic devices has led to supraharmonic issues.The concept of harmonic groups has been widely used to minimize energy leakage. Moreover, the distribution of supraharmonics is related to the switching frequency of harmonic sources. Given the diversity of switching frequencies and emissions distribution, harmonic groups need to be flexibly adjusted. A switching frequency identification method based on correlation analysis is proposed in this work. In addition, the switching frequencies of supraharmonic sources are identified through a correlation analysis of the supraharmonic emissions of a measurement point. Furthermore, a flexible supraharmonic group method in which bandwidth can be adjusted according to switching frequency is proposed. This method can avoid inconsistency between the emissions and group centers and minimizes energy leakage successfully. Finally, the method is validated via simulation and test data.

INDEX TERMS Supraharmonic, switching frequency, harmonic group,data identification.

I. INTRODUCTION

The switching frequency of power electronic devices continues to increase with the development of power electronic devices, thereby leading harmonic injection to extend to high frequencies. High-frequency harmonics can cause electrical device malfunction or damage [1]–[3], power-line data transformer errors [4], [5], and power-metering errors which have resulted in the rapid development of a new power-quality issue [6], [7]. In 2013, the 2–150kHz high-frequency component of the power system is first defined as supraharmonic [8].

The concept of harmonic groups is generally used in traditional harmonic analysis. When a signal contains a fundamental component and/or harmonics with fluctuating amplitudes, the energy of the components will diffuse into adjacent frequency components, and estimation accuracy can be improved by harmonic group parameters [9], [10]. The IEC 61000-4-7 [11] standards point out that a harmonic group can aggregate emitted energy, minimize spectrum leakage effectively, and improve spectral analysis accuracy [13]. In addition, harmonic group calculation can be used to evaluate the degree of harmonic distortion [12].

Two kinds of harmonic grouping standards are available in the current standards. The grouping bandwidth is 200Hz in the IEC 61000-4-7 [11], [14], [15] and the CISPR 16-2-1 standards, while that in the IEC 61000-4-30 [16] standard is 2kHz. The IEC 61000-4-7 and IEC 61000-4-30 standards are used for unintentional emission in the frequency range of 2-9kHz and 9-150kHz, while the CISPR 16-2-1 [17] standard is used for intentional emissions in the frequency range of 9kHz–30 MHz.This study mainly focuses on unintentional emissions.

Bandwidth is an important factor that affects the measurement accuracy, different bandwidth leading to differences in frequency signal components inconsistently [18].For example, when the bandwidth is 200Hz and 2kHz,the differences of the measure result to PLC(Power Line Communication) signals, background noises and other broadband emission may over 10dB μV [19], [20]. The above standards using 9kHz as dividing line in the range of 2-150kHz, setting bandwidth of 200Hz and 2kHz respectively, which increase the difference between the result and bring inconvenience to the emission analyzing. In this case, the bandwidth consistency between harmonic group is necessary [20]. In addition, due to

The associate editor coordinating the review of this manuscript and approving it for publication was Jing Liang.

the wide frequency band features of supraharmonics, the size of bandwidth should also be reconsidered, which should be greater than 600Hz for some experts [21].

In contrast to low-frequency harmonics, the distribution of supraharmonics is closely related to the switching frequency of power electronic devices and considerably varies between different switching frequencies [4].The diversity of the switching frequency contributes to a wide range of frequency distributions, from several kilohertz to hundreds of kilohertz, with a strong randomness of distribution [22]. The grouping effect of the above standards differs when dealing with different switching frequencies. Thus, a harmonic group method should consider the switching frequency. However, during analysis, the switching frequencies of supraharmonic sources are generally unknown, thereby complicating the analysis of emissions features. Accurately identifying the switching frequencies of supraharmonic sources in power grids can provide a reference for harmonic group methods and for effectively distinguishing different harmonic source emissions, which are helpful for analyzing supraharmonic emissions and studying the interaction between these emissions in different equipment.

The contributions of this study are as follows:

1) A switching frequency identification method is proposed on the basis of correlation analysis to analyze the emission features of supraharmonics.

2) A flexible supraharmonic group method that considers the emission features of supraharmonics and the selection of bandwidth according to the switching frequencies of harmonic sources is proposed to evaluate supraharmonic emissions.

These methods are verified through extensive simulation and test.

II. IDENTIFICATION OF SWITCHING FREQUENCY

A. PRINCIPLE OF CORRELATION ANALYSIS

The similarity measure is a quantitative parameter that is used to depict or explain the degree of similarity between matching entities. Generally, degree of similarity is calculated by the cost function. The cost function is designed to match the numerical function in a physical space, and the co-equivalent entity with the same name is determined according to the numerical value calculated by the cost function of different matching entities. Common cost functions include the distance function and direction function. In this work, the Pearson correlation coefficient is used to calculate the cosine angle of the space vector based on the general normalization of vectors X and Y, as shown in (1). The direction consistency between X and Y can be quantified by calculating the similarity coefficient.

$$r = \frac{\mathrm{cov}(X, Y)}{\sigma_X \sigma_Y} = \frac{\sum_{i=1}^{n} (X_i - \bar{X})(Y_i - \bar{Y})}{\sqrt{\sum_{i=1}^{n} (X_i - \bar{X})^2} \sqrt{\sum_{i=1}^{n} (Y_i - \bar{Y})^2}} \quad (1)$$

In the formula, Cov(X, Y) are the covariance's of X and Y; and σ_Y are the standard deviations of X and Y, respectively; X_i, Y_i are the elements in vector X, Y; and $\overline{X}$ and $\overline{Y}$ are the average values of the elements in vectors X and Y, respectively.

The theoretical spectrum of supraharmonic emissions can be obtained through the double-Fourier calculation of power electronic devices under PWM modulation [23]. Subsequently, correlation between the spectrum diagram and actual supraharmonic emissions is analyzed, and switching frequency can be identified by matching the variation law. However, the law of supraharmonic spectrum distribution is affected by switching frequency, the maximum amplitude positions at different switching frequency are inconsistent, and correlation analysis cannot be conducted directly. Therefore, this work proposes the following algorithm for switching frequency identification.

B. SWITCHING FREQUENCY IDENTIFICATION ALGORITHM

Switching frequency identification is divided into three steps. First, a theoretical spectrum is obtained through double-Fourier calculation, and feature components are extracted to form the reference feature component vector A (named as the feature component behind, the form method is described below) .Second, based on the test data, all frequency values that may be related to switching frequency are extracted. These values are assumed to be the switching frequency in turn, and the feature component B_i, C_j is formed by extracting the associated component from the spectrum. Finally, correlation between vector B_i, C_j and vector A is analyzed, and the actual switching frequency is identified according to the correlation coefficient. In the following section, extraction of the component associated with switching frequency and formation of the feature component are described in detail.

1) ASSUMED SWITCHING FREQUENCY EXTRACTION

To avoid the influence of low-frequency harmonics, the low-frequency component must first be filtered. Supraharmonics are mainly distributed at approximately one or two switching frequencies. Harmonic sources with switching frequencies exceeding 1kHz have important emissions in the range of 2–150kHz. Therefore, the frequency range of 1–150kHz is used to identify switching frequencies greater than 1kHz. Without considering interference, the maximum amplitude of supraharmonic emissions generally occurs when the frequency is the switching frequency [7] (Fig. 1 (a)), or the symmetrical sideband is either centered on the switching frequency or an integer multiple of the switching frequency [24] (Fig. 1 (b)). Therefore, the extraction range is divided into two parts: 1) the corresponding frequency of large-amplitude components in the spectrum analysis. The larger the number of components selected, the smaller the influence of noise on the analysis results but the larger the computation amount. In this case, the frequencies of the first 20 maximum amplitude components are selected. 2) If the interval between any two components that originate from 1) are $2f_c$, $4f_c$, $6f_c$, or

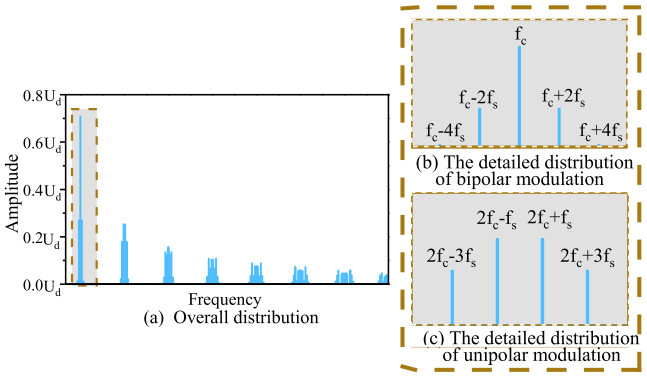

FIGURE 1. Distribution of supraharmonics.

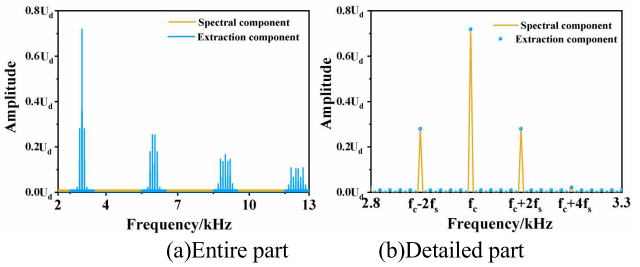

FIGURE 2. Conceptual diagram of feature component extraction.

$8f_c$(Fig. 1 (c)), then the average and 1/2 average values are selected.

2) STRUCTURE OF FEATURE COMPONENTS

In addition to switching frequency, the control mode, modulation ratio, DC side voltage/current, and fundamental frequency will affect supraharmonic distribution. The influence of the above factors must be excluded to identify switching frequency accurately. In this work, the influences of the switching frequency and the fundamental frequency on the distribution are eliminated by forming feature components.

According to the PWM formula (the SPWM formula is taken as an example, see Formula (2)), supraharmonic emissions, which are PWM, have the following features. 1) They are mainly distributed around the switching frequency f_c and its integer in the spectrum, and the amplitude decreases gradually with an increase in frequency. Maximum amplitudes generally appear around the switching frequency (or double-switching frequency). 2) All emissions are centered on the switching frequency f_c and its integer multiples, and the amplitude is symmetrically distributed. 3) All emissions around the switching frequency f_c and its integer multiples spacing multiples fundamental frequency f_s that is, the emissions only occur when the frequency is $mf_c \pm nf_s$, where m is a positive integer, n is 0, 1, 2....

$$\begin{aligned} u(t) = {} & \mathrm{M}U_\mathrm{d} \sin 2\pi f_s t \\ & + \frac{4U_\mathrm{d}}{\pi} \sum_{m=1,3,5,L}^{\infty} \frac{J_\mathrm{n}(\frac{mM\pi}{2})}{m} \sin \frac{m}{2}\pi \cos(m2\pi f_c t) \\ & + 4\frac{U_d}{\pi} \sum_{m=1,2,L}^{\infty} \sum_{m=\pm1,\pm2,L}^{\pm\infty} \frac{J_\mathrm{n}(\frac{mM\pi}{2})}{m} \sin(\frac{m+n}{2}\pi) \\ & \times \cos(m2\pi f_c t + n2\pi f_s t - \frac{n\pi}{2}) \end{aligned} \quad (2)$$

In the above formula, U_d is the DC side voltage, M is the modulation factor, J_n is the Bessel function, and other parameters are the same as above. According to the features above, components with a frequency of $mf_c \pm nf_s$(designated as the feature frequency in the following sections) must be included when forming the feature component. However, as a result of the large differences in switching frequency between different devices, neglecting the value of f_c, f_s and replacing it with m, n is convenient. The value of m, n can be infinite in actual situations, whereas emissions decrease as frequency increases. To save computation time, m is taken as 1–10 and n as 0–10, which have negligible influences on the identification result.

Formula (3) shows the structure of the feature component, and the amplitude-corresponding frequency is the element in the vector. Figures 2 (a) and (b) show conceptual diagrams of feature component extraction, where the blue region is the extraction part.

$$\begin{aligned} B_\mathrm{i}, C_\mathrm{j} = {} & (mag_{\mathrm{f_r}-(\mathrm{N}-1/\mathrm{e})\mathrm{f_c}}, mag_{\mathrm{f_r}-(\mathrm{N}-2/\mathrm{e})\mathrm{f_c}} \\ & \cdots mag_{\mathrm{f_r}-(\mathrm{N}-((\mathrm{eN}-1)/\mathrm{e})\mathrm{f_c}}, mag_{\mathrm{f_r}}, mag_{\mathrm{f_r}+1/\mathrm{ef_c}} \\ & \cdots mag_{\mathrm{f_r}+\mathrm{Nf_c}}, mag_{2\mathrm{f_r}-\mathrm{Nf_c}}, mag_{\mathrm{Qf_r}+\mathrm{Nf_c}})^\mathrm{T} \end{aligned} \quad (3)$$

In the above formula, mag_l is the amplitude of frequency l, N is the number of extracted sidebands, e is the number of sampling points between every feature component (in this paper, $e = 4$), f_r is the assumed switching frequency, f_c is the modulation wave frequency, and Q is the extraction switching frequency multiple of the construction vector.

Construction of the reference feature component A is similar to the method above, and the formula is the same as Formula (3). However, only one feature component needs to be constructed. In addition, according to the double-Fourier calculation formula, the switching frequency, the fundamental frequency, the modulation coefficient, and the DC side voltage should be assumed in advance. Switching frequency and fundamental frequency parameters are replaced in the feature component extraction process, which will not affect the identification result. The DC side voltage only affects the overall amplitude of the harmonics but not the spectrum distribution. That is, it has no influence on the identification result. The modulation coefficient has a negligible effect on the correlation calculation result and does not affect the identification result, because the identification result is available only when all the correlation coefficients are compared.

3) COMPUTATION

This method can identify switching frequency according to the supraharmonic distribution law and possesses satisfactory anti-noise capabilities. Figure 3 (in appendix) shows

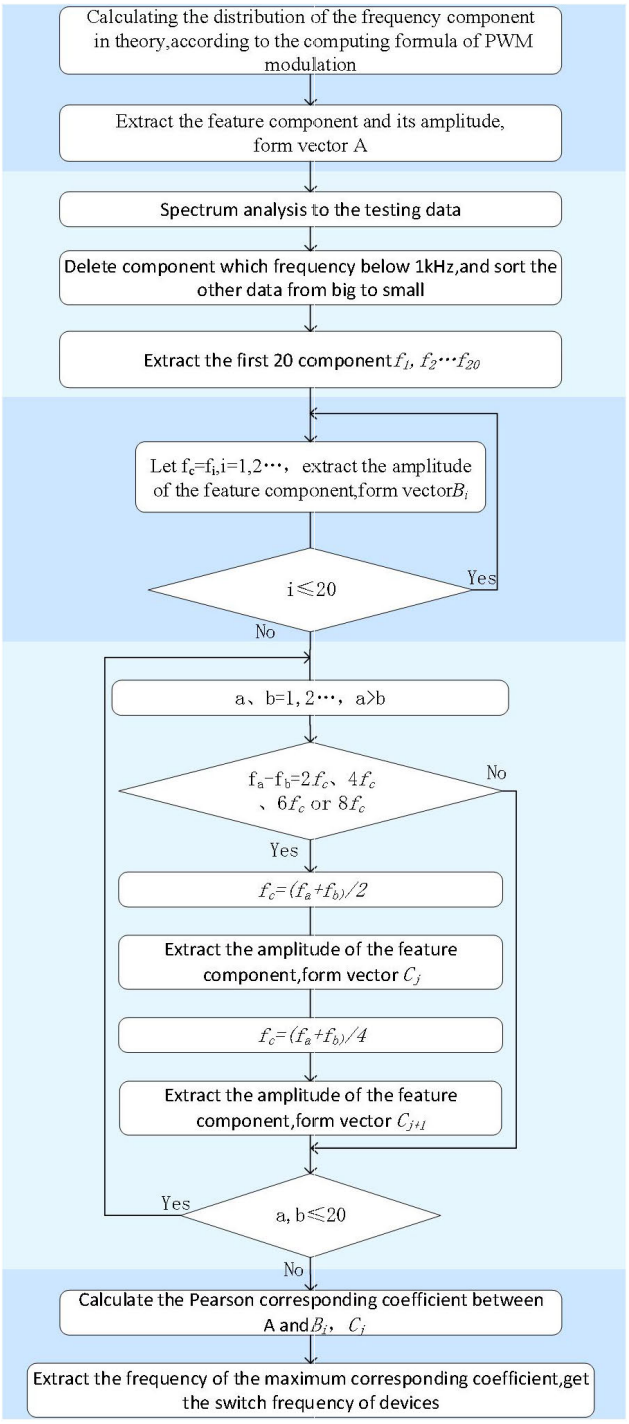

FIGURE 3. The process of switching frequency identification.

the proposed switching frequency identification method. This method is applicable to the switching frequency identification of the PWM with a known harmonic source control mode. If the control mode is unknown, it can be identified by setting a spectrum distribution database of different control modes. Then, the switching frequency can also be identified.

TABLE 1. Average energy leakage of supraharmonics.

Sideband energy /associating peak energy (%)		Multiples of the switching frequency									
		1	2	3	4	5	6	7	8	9	10
Δf	f_s、$2f_s$	46.0	49.1	53.0	49.5	52.0	50.0	77.5	50.0	79.9	50.0
	$3f_s$、$4f_s$	29.8	34.1	45.2	34.2	26.7	47.7	59.0	55.0	77.3	60.5
	$5f_s$、$6f_s$	29.6	24.4	9.7	26.9	30.5	13.5	50.0	34.6	85.1	60.2
	$7f_s$、$8f_s$	3.7	18.2	38.9	20.1	27.8	34.3	73.3	10.0	55.9	39.8
	$9f_s$、$10f_s$	2.8	5.3	23.0	19.1	28.5	31.3	45.6	66.9	70.9	44.3
	$11f_s$、$12f_s$	2.0	2.5	20.2	20.0	3.6	7.6	24.9	52.2	60.3	66.5
	$13f_s$、$14f_s$	1.8	1.5	24.6	21.4	18.2	1.1	4.6	18.7	55.9	81.2
	$15f_s$、$16f_s$			4.0	30.1	10.1		0.6	4.1	14.7	40.0
	$17f_s$、$18f_s$	-	-	2.2	24.5	7.8	-	-	0.6	2.7	12.0
	$19f_s$、$20f_s$			4.8	2.0	4.6			-	-	2.5
Associating peak energy/ the switching frequency emission (%)		-	78.9	31.9	45.5	26.7	36.1	16.0	21.5	9.0	5.8

III. FLEXIBLE HARMONIC GROUP METHOD

Power electronic devices inevitably produce nonlinear waveforms from switching on and off. Subsequently, energy is leaked to the switching frequency (and its multiples), and sideband frequencies in the spectrum analysis and supraharmonics are generated [21]. The harmonic grouping method should account for harmonic emissions features, and bandwidth selection should consider the leakage feature of the harmonics. Thus, grouping most of the associating energy together would be an ideal situation. For example, low frequency harmonics are centered on the maximum amplitude, thereby grouping the energy around a bandwidth,and the interharmonics group the energy between two harmonic emissions [11]. To minimize energy leakage, energy is aggregated by grouping it around multiple switching frequencies, which is consistent with the aforementioned idea.

A. BANDWIDTH SELECTION

As inferred from supraharmonic emissions features in Section II, the distance between each adjacent sideband and the switching frequency f_c (as well as its multiples, which are called center frequencies) is multiples of the fundamental frequency f_s. Table 1 summarizes the average energy leakage of several common supraharmonic emissions sources, including a photovoltaic inverter, a fan converter, a frequency converter, and a static var generator (SVG), which is the ratio

TABLE 2. Comparison of different bandwidth aggregation effects.

Group range	Aggregate emission/Total emission (%)
f_c-2f_s~f_c+2f_s	26.5
f_c-4f_s~f_c+4f_s	46.5
f_c-6f_s~f_c+6f_s	61.1
f_c-8f_s~f_c+8f_s	72.4
f_c-10f_s~f_c+10f_s	81.9
f_c-12f_s~f_c+12f_s	88.6
f_c-14f_s~f_c+14f_s	94.2
f_c-16f_s~f_c+16f_s	97.4
f_c-18f_s~f_c+18f_s	99.5
f_c-20f_s~f_c+20f_s	100.0

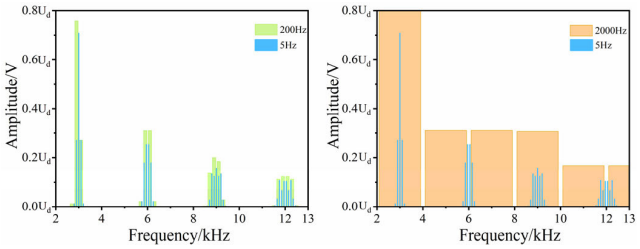

(a) 200Hz (b)2000Hz

FIGURE 4. 200Hz, 2000Hz grouping effect diagram.

of the sideband harmonic amplitude to the center frequency harmonics. Δf is the difference between the sideband harmonic and its corresponding center frequency as follows, where N=1,2,…, f is the the frequency of every emission.

$$\Delta f = \min\{f - Nf_c\} \tag{4}$$

Given supraharmonic emissions features, the same central frequency sideband harmonic emissions is generally odd or only even. The two adjacent sidebands are shown together in Table 1.

Bandwidth has a considerable influence on the accuracy of supraharmonic measurement [18], [19]. Fig. 4 compares the different bandwidth aggregation effects of theoretical spectrum data (switching frequency is 3kHz) under two non-intentional emissions standards in which 5Hz components are the original spectra, and the 200 and 2000Hz components (resolution is 200Hz/2000Hz) are the spectra after grouping, according to the standards of IEC 61000-4-7 and IEC 61000-4-30, respectively. In the case of $f_s = 50$Hz, the 200Hz bandwidth can cover only the four sidebands, that is, $mf_c \pm z_s$ and $mf_c \pm 2f_s$, simultaneously, which is insufficient for covering the main energy of one emissions band. Table 2 shows the percentage of energy grouping under different bandwidths according to Table 1. Table 2 shows that the 200Hz bandwidth can group only 26.5% of the energy. Thus, a large energy leakage can be observed outside this range, as verified in Fig. 4 (a).

In addition, owing to the attenuation features of sideband harmonics, the farther the distance between the sideband frequency emissions to the center, the smaller the amplitude and the higher the noise ratio. As seen from Fig. 4 (b), most of the supraharmonic main emissions bandwidth is considerably less than 2000Hz. Moreover, the 2000Hz bandwidth covers the frequency of $mf_c \pm f_s$, $mf_c \pm 2f_s \ldots mf_c \pm 20f_s$ simultaneously, that is, 40 sidebands in total. This coverage is excessively large and can lead to a low signal-to-noise ratio in actual tests. For example, in Table 1, because the amplitude of the partial harmonic emissions is small, emissions cannot be judged under noise interference, and the statistical data are vacant. This phenomenon is evident at frequency of $mf_c \pm 15f_s$(corresponding bandwidth 1500Hz). To summarize, bandwidth should be between 200 and 1500Hz.

Subsequently, with an increase in switching frequency multiples, energy leakage and attenuation tend to be severe. The flexible harmonic group method aims to minimize energy leakage by more than 70%. Approximately 72.4% of energy can be grouped when bandwidth is larger than 800Hz (the grouping range is mf_c-$8f_s$ ~mf_c+$8f_s$; see Table 2, where the specific group effect is based on the results of the actual analysis). Based on the above analyses, the harmonic range is larger than mf_c-$8f_s$ ~mf_c+$8f_s$ but smaller than mf_c-$15f_s$ ~mf_c+$15f_s$, the bandwidth range is as follows:

$$800\ Hz \leq b \leq 1500\ Hz \tag{5}$$

B. FLEXIBLE SUPRAHARMONIC GROUPING METHOD

The existing data consider the center of the emissions frequency band as the center frequency. However, in practical applications, this requirement is not always satisfied. In the above standards, bandwidth is generally decided first, and the group is formed from small to large according to frequency. This method will result in the grouping of a large number of sideband emissions into another center frequency, and the consistency between the emissions center and the group center cannot be guaranteed, as shown in Fig. 4 (b).

Thus, a flexible supraharmonic grouping method is proposed to maintain consistency between the emissions and group centers. The position of the center band is determined first, and bandwidth b, which can be adjusted according to the switching frequency of the devices in certain ranges, is determined. The detailed steps are as follows. Bandwidth b is assumed first, then all the group centers are ensured as the center frequency. To meet the requirements, the number of the group between the two adjacent center frequencies should be an integer, that is, f_c/b is an integer. Then, bandwidth b is determined according to the requirement in Part III,Section A, that is, bandwidth should be between 800 and 1500Hz. Finally, the group starts from the switching frequency and its two sides. Fig. 5 superimposes the spectrum diagram before and after grouping and illustrates the group boundaries (the black columnar portion considering the resolution of the spectrum analysis) and its corresponding relationships, where F is the central frequency of each group; the blue and black

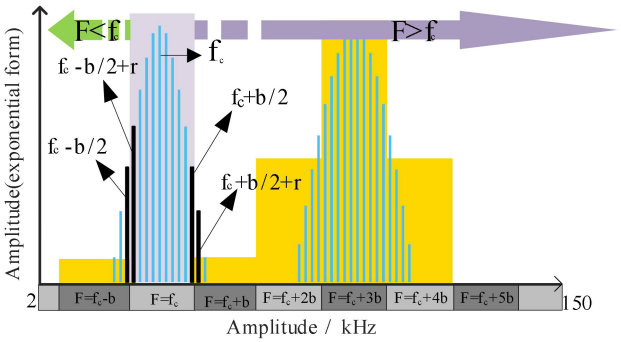

FIGURE 5. Schematic diagram of supraharmonic group method.

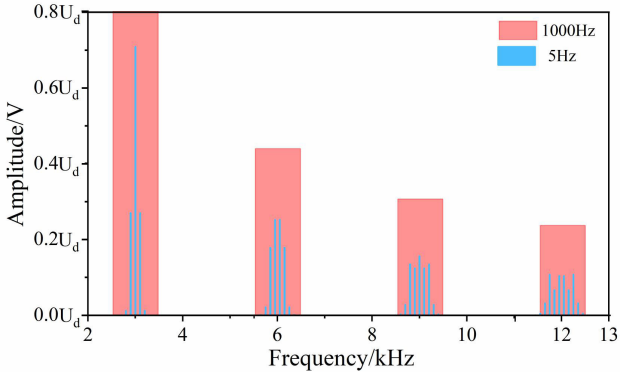

FIGURE 6. The effect of flexible supraharmonic grouping method.

rectangles are the spectrum before grouping, with a resolution of 5Hz; and the yellow and pink rectangles are the spectra after grouping, with a resolution of b.

The amplitude of the harmonic group defined in IEC 61000-4-7:2002 is the root mean square of the effective value of a harmonic and its adjacent spectral components. In reference to the calculation method in IEC 61000-4-7 and Fig.5, the amplitude after grouping is represented by $G_{b,F}$, where b is the bandwidth. When the center frequency of the group is the switching frequency, that is, $F = f_c$ (the pink rectangular part of the figure), the amplitude calculation after grouping is

$$G_{b,F} = \sqrt{\sum_{f=f_c-b/2+r}^{f=f_c+b/2} Y_f^2} \tag{6}$$

In the above formula, f is the frequency before grouping, Y_f is the corresponding amplitude, r is the resolution of the spectrum before grouping, and the following formula is the same. When the center frequency is less than the switching frequency, that is

$$2000 \le F = f_c - mb < f_c \quad m = 1, 2, \cdots \tag{7}$$

(the green arrow in the figure), the amplitude calculation after grouping is

$$G_{b,F} = \sqrt{\sum_{f=f_c-(2m+1)b/2+r}^{f=f_c-(2m-1)b/2} Y_f^2} \tag{8}$$

When the center frequency is larger than the switching frequency, that is

$$f_c < F = f_c + sb, \quad s = 1, 2, \cdots \tag{9}$$

(the purple arrow in the figure), the amplitude calculation after grouping is

$$G_{b,F} = \sqrt{\sum_{f=f_c+(2s-1)b/2+r}^{f=f_c+(2s+1)b/2} Y_f^2} \tag{10}$$

According to the method mentioned above, the spectrum in Fig. 4 shows a grouping (Fig. 6) in which 1kHz is

TABLE 3. The effect of energy grouping.

Frequency	Percentage			Total emission/V
	200Hz	2000Hz	1kHz	
f_s	94.18%	100.00%	100.00%	8.05
$2f_s$	70.54%	70.71%	100.00%	4.38
$3f_s$	65.37%	100.00%	100.00%	3.06
$4f_s$	52.27%	70.71%	100.00%	2.36
$5f_s$	55.34%	100.00%	99.94%	1.92
$6f_s$	49.46%	70.71%	99.70%	1.62
$7f_s$	45.89%	100.00%	95.80%	1.39
$8f_s$	42.60%	70.71%	89.28%	1.22
$9f_s$	40.47%	100.00%	79.21%	1.07
$10f_s$	33.93%	70.71%	72.27%	0.95
Average value	**55.00%**	**85.36%**	**93.62%**	

the bandwidth selected through the flexible supraharmonic group method based on actual emissions. A comparison of Figs. 4 and 6 reveals that the latter group has high energy and avoids the inconsistency between the emissions center and the group center. Table 3 compares the effects of the energy grouping in Figs. 4 and 6. The flexible supraharmonic group method can group 93.62% of the energy of 1–10 times the switching frequency, which is better than 55% and 85.36% for the other methods shown in Fig. 1.

The switching frequency of harmonic sources must be initially identified in the flexible supraharmonic group method. Therefore, the entire flow-process diagram of the supraharmonic analysis is shown in Fig. 7 in the Appendix, where the purple square is the study range of this paper.

IV. SIMULATION AND EXPERIMENTAL VERIFICATION

The simulation and test data are taken as examples to verify the effectiveness of the proposed method.

A. SIMULATION DATA VERIFICATION

The output waveform on the grid-connected side of an SVG simulation model is used. The model is controlled by

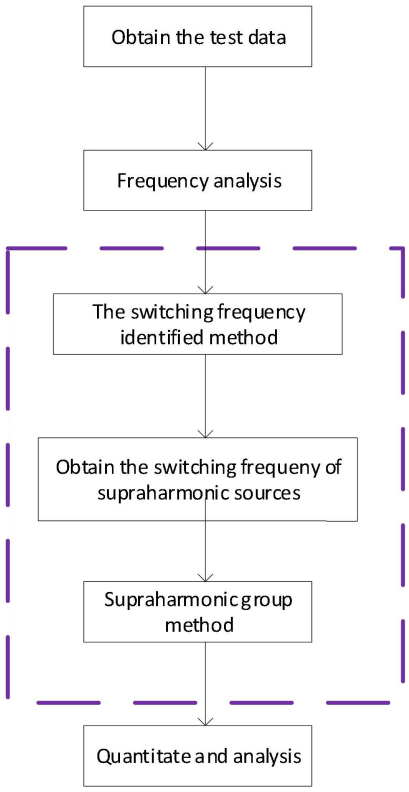

FIGURE 7. Supraharmonic analysis flow-process diagram.

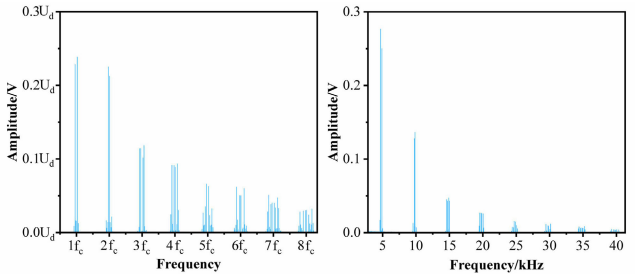

(a) Theory spectrum (b) Test spectrum

FIGURE 8. Theory and simulation spectrum of SVG.

SVPWM, the waveform is sampled for 1 s, the spectrum is analyzed for 10 cycles, and the sampling frequency is 1 MHz.

1) THE SWITCHING IDENTIFICATION METHOD

Switching frequency identification is mainly divided into three steps: ① spectrum analysis, ② feature component extraction, and ③ correlation analysis and switching frequency identification.

① Spectrum analysis

First, the theoretical spectrum (see Fig. 8 (a)) is obtained according to the SVPWM double-Fourier transform formula [19]. Next, the simulation data spectrum is obtained via fast Fourier transform (Fig. 8 (b)). Finally, frequencies corresponding to the first 20 maximum amplitudes are extracted according to the results of the spectrum analysis (see Table 4 in appendix).

TABLE 4. The 20 maximum amplitudes and its frequency.

Amplitude/V	Frequency/kHz	Amplitude/V	Frequency/kHz
0.2764	4.9	0.026	20.05
0.2501	5.1	0.0256	20.25
0.1363	10.05	0.0168	4.8
0.1277	9.95	0.0153	24.9
0.0473	15.1	0.0147	25.1
0.0449	14.8	0.0129	9.75
0.0428	15.2	0.0118	30.35
0.0426	14.9	0.0113	29.65
0.0267	19.75	0.0105	10.045
0.0265	19.95	0.0102	9.955

TABLE 5. Correlation coefficient of the hypothetical frequency.

Switching frequency/kHz	Correlation coefficient	Switching frequency/kHz	Correlation coefficient
5	0.7012	7.475	0.2922
7.425	0.4396	15.2	0.2715
19.85	0.4346	19.75	0.2675
34	0.4208	17.425	0.2581
14.9	0.4198	12.575	0.2569
17.275	0.4031	14.8	0.2559
15.1	0.3881	9.75	0.2118
17.325	0.3347	20.25	0.2067
20.05	0.3171	4.9	0.1504
19.95	0.3164	17.475	0.1484

② Feature component extraction

The feature component extraction process is shown in Fig. 3(in appendix). First, the feature component is extracted from the theoretical frequency spectrum, and vector A is formed. Next, every frequency in Table 4 is assumed to be the switching frequency, and feature components are extracted to form vector B_i, i = 1,2…20. Finally, every two components with a frequency interval of $2f_c$, $4f_c$, or $6f_c$ are extracted and their average frequency is calculated. Half, which is assumed to be the switching frequency and the feature components, is extracted, that is, vector C_j, j = 1,2…31.

③ Correlation analysis and switching frequency identification

Table 5 (in appendix) shows the correlation analysis between A and every B_i and C_j, the correlation coefficient, and the switching frequency that corresponds with the maximum correlation coefficient. According to the above process, the switching frequency of SVG is 5kHz, which is consistent with the set value.

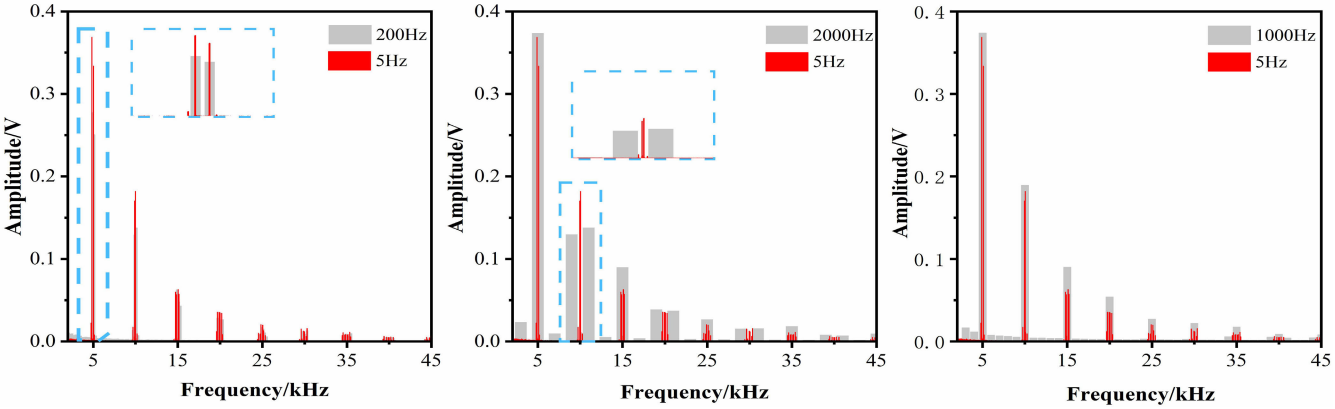

(a) IEC 61000-4-7 (b) IEC 61000-4-30 (c) The flexible supraharmonic group method

FIGURE 9. The group spectrum of simulation data with different method.

TABLE 6. The effect of grouping.

Frequency	Bandwidth			Total emission/V
	200Hz	2000Hz	1000Hz	
f_s	74.05%	99.85%	99.82%	3.742
$2f_s$	72.62%	72.77%	99.87%	1.893
$3f_s$	69.39%	99.80%	99.73%	0.901
$4f_s$	49.42%	72.25%	99.62%	0.539
$5f_s$	62.95%	99.25%	98.75%	0.270
$6f_s$	42.74%	71.43%	98.58%	0.223
$7f_s$	47.26%	99.14%	94.37%	0.185
$8f_s$	35.68%	73.62%	77.50%	0.109
$9f_s$	46.41%	98.12%	85.47%	0.095
$10f_s$	22.99%	72.04%	64.05%	0.083
Average value	**52.35%**	**85.83%**	**91.78%**	

In addition, Gaussian white noise is added to the waveform, and the immunity of the parameter identification algorithm is verified. The method possesses satisfactory noise immunity. A signal-to-noise ratio of –15 dB can still identify switching frequency accurately.

2) FLEXIBLE SUPRAHARMONIC GROUPING METHOD

As previously mentioned, the switching frequency of the supraharmonic source is 5kHz.

The flexible supraharmonic grouping method states that bandwidth should be 1kHz. Figures 9 (a), (b), and (c) show the frequency spectrum diagram after grouping, according to the standards of the IEC 61000-4-7 and the IEC 61000-4-30 and the flexible supraharmonic group method, respectively. A comparison of Fig. 9 reveals that the flexible supraharmonic grouping method groups energy well and effectively minimizes energy leakage, which is consistent with actual

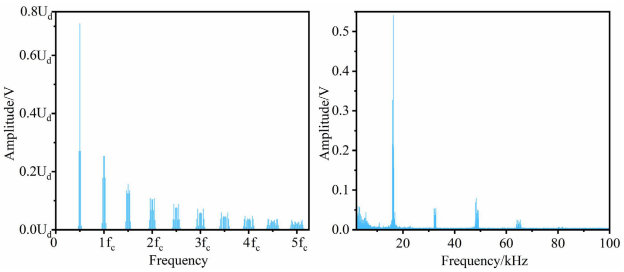

(a) Theory spectrum (b) Test spectrum

FIGURE 10. Photovoltaic inverter theory and test spectrum.

emissions. Table 6 (in appendix) compares the effects of three grouping methods. The flexible grouping method can group 91.78% of 1–10 times the emissions of switching frequency. This value is larger than 52.35% and 85.83% of the other two standards. Thus, the grouping effect has improved drastically.

B. TEST DATA VERIFICATION

To verify the feasibility of the method described in this paper in practical applications, the grid-side voltage data of a 36kVA photovoltaic inverter are analyzed. The control mode adopts bipolar SPWM and test waveform sampling for 2 s. It takes 10 cycles of data for analysis, and the sampling frequency is 500kHz.

1) SWITCHING IDENTIFICATION METHOD

The steps of switching frequency identification are consistent with the case above, and the bipolar SPWM theoretical spectrum calculation formula is used (Fig. 10 (a); the real spectrum is shown in Fig. 10 (b)). Table 7 (in appendix) shows the first 20 maximum amplitudes according to the results of the spectrum analysis, and the correlation coefficients are shown in Table 8(in appendix). According to switching frequency identification, the switching frequency of the photovoltaic inverter is 16.25kHz, which is consistent with the follow-up analysis (not shown in this paper).

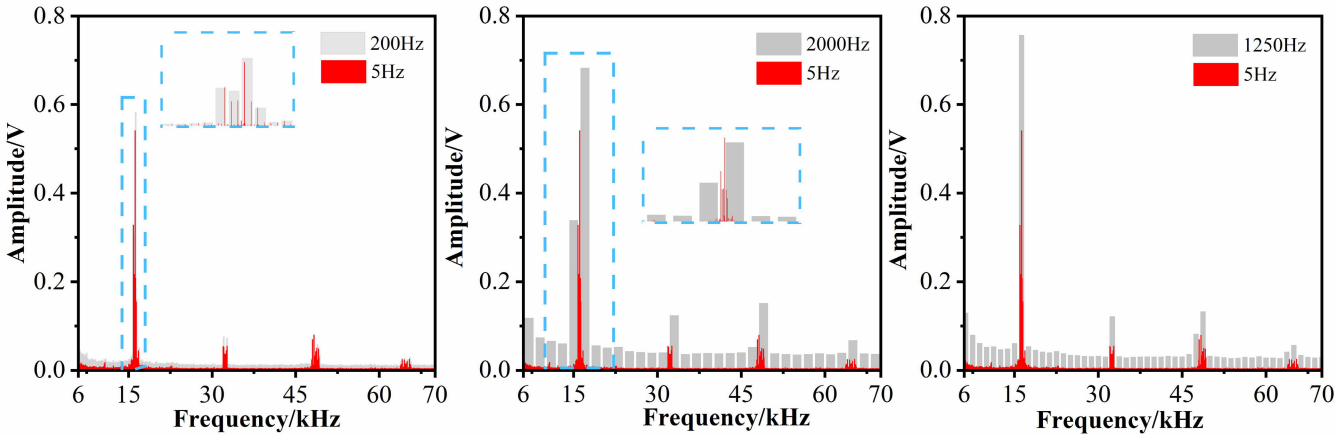

(a)IEC 61000-4-7 (b) IEC 61000-4-30 (c) The flexible supraharmonic group method

FIGURE 11. Spectrum of simulation data grouped with different method.

TABLE 7. The 20 maximum amplitudes and its frequency.

Amplitude/V	Frequency/kHz	Amplitude/V	Frequency/kHz
0.54	16.25	0.057	3.25
0.327	15.96	0.054	32.76
0.216	16.16	0.053	32.06
0.21	16.06	0.052	32.16
0.207	16.36	0.05	48.87
0.154	16.46	0.048	49.17
0.079	48.37	0.047	3.26
0.069	48.07	0.044	16.21
0.06	2.25	0.044	32.66
0.058	2.95	0.044	16.86

TABLE 8. Correlation coefficient of the hypothetical frequency.

Switching frequency/kHz	Correlation coefficient	Switching frequency/kHz	Correlation coefficient
16.25	**0.719**	6.055	0.438
48.065	0.617	16.355	0.417
16.155	0.613	15.955	0.404
16.155	0.613	3.25	0.363
32.76	0.601	2.25	0.337
48.365	0.546	48.865	0.335
32.06	0.521	2.95	0.317
32.66	0.491	16.245	0.257
32.16	0.479	16.455	0.184
49.165	0.466	16.855	0.155

2) THE FLEXIBLE SUPRAHARMONIC GROUPING METHOD

According to the above identification, the switching frequency of the PV inverter is 16.25kHz. Based on the flexible supraharmonic grouping method, bandwidth should be 1.25kHz. Figs. 11 (a), (b), and (c) show the spectrum after grouping, according to the standards of the IEC 61000-4-7 and the IEC 61000-4-30 and the flexible supraharmonic group method, respectively. A comparison of Figure 11 shows that the flexible supraharmonic grouping method has better reduction abilities and minimizes energy leakage better than other methods.

V. CONCLUSION

A switching frequency identification method that can identify the switching frequency of a supraharmonic source at a test point is proposed in this work. In addition, the proposed method can eliminate the influence of noise and other interferences based on the emissions law of supraharmonics.

On this basis, a flexible supraharmonic grouping method, in which bandwidth can be adjusted in accordance with the switching frequency of supraharmonic sources, is proposed. This method can efficiently show the supraharmonic emission feature and achieve effective data compression. The bandwidth is also decided by the sideband width centered on the switching frequency, which is helpful for setting the filter range specifically. Considering the discrete distribution feature of supraharmonics, the comparison among different facilities should mainly focus on the switching frequency and its multiples rather than the same frequency.

The proposed method is verified using simulation and test data, and a satisfactory effect is obtained. The analysis results show that the switching frequency identification method has good immunity and can identify switching frequency accurately even under severe noise. Compared with existing standards, the flexible supraharmonic grouping method improves the percentage of energy grouping and achieves better grouping effects.

APPENDIX

See Figs. 3 and 7 and Tables 4 to 8.

ACKNOWLEDGMENT

The authors gratefully acknowledge the contributions of H. Yao for his work on providing testing facilities.

REFERENCES

[1] *Study Report on Electromagnetic Interference Between Electrical Equipment/Systems in the Frequency Range Below 150 kHz*, Irish Standard Recommendation S.R. CLC/TR 50627:2015, CENELEC, 2015.

[2] J. Meyer, S. Haehle, and P. Schegner, "Impact of higher frequency emission above 2 kHz on electronic mass-market equipment," in *Proc. 22nd Int. Conf. Exhibit. Electr. Distribution (CIRED)*, Stockholm, Sweden, 2013, pp. 1–4.

[3] T. Wohlfahrt, C. Waniek, J. M. A. Myrzik, J. Meyer, and P. Schegner, "Supraharmonic disturbances: Lifetime reduction of electronic mass-market equipment by the aging of electrolytic capacitors," in *Proc. 18th Int. Conf. Harmon. Qual. Power (ICHQP)*, Ljubljana, Slovenia, May 2018, pp. 1–6.

[4] A. Gil-de-Castro, S. K. Ronnberg, and M. H. J. Bollen, "A study about harmonic interaction between devices," in *Proc. 16th Int. Conf. Harmon. Qual. Power (ICHQP)*, Bucharest, Romania, May 2014, pp. 728–732.

[5] S. K. Ronnberg, M. H. J. Bollen, and M. Wahlberg, "Interaction between narrowband power-line communication and end-user equipment," *IEEE Trans. Power Del.*, vol. 26, no. 3, pp. 2034–2039, Jul. 2011.

[6] D. Amaripadath, R. Roche, L. Joseph-Auguste, D. Istrate, D. Fortune, J. P. Braun, and F. Gao, "Power quality disturbances on smart grids: Overview and grid measurement configurations," in *Proc. 52nd Int. Univ. Power Eng. Conf. (UPEC)*, Heraklion, Greece, Aug. 2017, pp. 1–6.

[7] P. M. Korner, R. Stiegler, J. Meyer, T. Wohlfahrt, C. Waniek, and J. M. A. Myrzik, "Acoustic noise of massmarket equipment caused by supraharmonics in the frequency range 2 to 20 kHz," in *Proc. 18th Int. Conf. Harmon. Qual. Power (ICHQP)*, Ljubljana, Slovenia, May 2018, pp. 1–6.

[8] A. Emanuel and A. McEachern, *Electric Power Definitions: A Debate*. Vancouver, BC, Canada: PES, 2013, pp. 21–25.

[9] H. Cheng Lin, "Inter-harmonic identification using group-harmonic weighting approach based on the FFT," *IEEE Trans. Power Electron.*, vol. 23, no. 3, pp. 1309–1319, May 2008.

[10] H. C. Lin, "Power harmonics and interharmonics measurement using recursive group-harmonic power minimizing algorithm," *IEEE Trans. Ind. Electron.*, vol. 59, no. 2, pp. 1184–1193, Feb. 2012.

[11] *Electromagnetic Compatibility (EMC)—Part 4-7: Testing and Measurement Techniques—General Guide on Harmonics and Interharmonics Measurements and Instrumentation, for Power Supply Systems and Equipment Connected Thereto*, Standard IEC 61000-4-7, 2008.

[12] M. Dalali and A. Jalilian, "Indices for measurement of harmonic distortion in power systems according to IEC 61000-4-7 standard," *IET Gener., Transmiss. Distrib.*, vol. 9, no. 14, pp. 1903–1912, Nov. 2015.

[13] I. Angulo, A. Arrinda, I. Fernandez, N. Uribe-Perez, I. Arechalde, and L. Hernandez, "A review on measurement techniques for non-intentional emissions above 2 kHz," in *Proc. IEEE Int. Energy Conf. (ENERGYCON)*, Leuven, Belgium, Apr. 2016, pp. 1–5.

[14] E. Gunther, "Harmonic and interharmonic measurement according to IEEE 519 and IEC 61000-4-7," in *Proc. IEEE/PES Transmiss. Distrib. Conf. Exhibit.*, Dallas, TX, USA, May 2006, pp. 223–225.

[15] P. Bilik, "Measurement of voltage and current harmonics for frequencies up to 9 kHz according to IEC61000-4-7," in *Proc. 10th Int. Conf. Electr. Power Qual. Utilisation*, Łódź, Poland, Sep. 2009, pp. 1–5.

[16] *Electromagnetic Compatibility (EMC)—Part 4-30: Testing and Measurement Techniques—Power Quality Measurement Methods*, Standard IEC 61000-4-30, 2015.

[17] *Specification for Radio Disturbance and Immunity Measuring Apparatus and Methods—Part 2-1: Methods of Measurement of Disturbances and Immunity—Conducted Disturbance Measurements*, Standard CISPR 16-2-1:2014, 2005.

[18] P. Verzele, J. Knockaert, and J. Desmet, "Appropriate methods to analyse power conversion harmonics," *Renew. Energy Power Qual. J.*, vol. 1, pp. 1271–1276, Mar. 2013.

[19] M. Klatt, J. Meyer, and P. Schegner, "Comparison of measurement methods for the frequency range of 2 kHz to 150 kHz," in *Proc. 16th Int. Conf. Harmon. Qual. Power (ICHQP)*, Bucharest, Romania, 2014, pp. 818–822.

[20] X. Xiao, K. Liao, S. Tang, and W. Fan, "Development of power electric system and new problems of supraharmonics," *Electrotech. Technol.*, vol. 33, no. 4, pp. 707–720, 2018.

[21] M. Klatt, J. Meyer, P. Schegner, A. Koch, J. Myrzik, G. Eberl, and T. Darda, "Emission levels above 2 kHz–laboratory results and survey measurements in public low voltage grids," in *Proc. 22nd Int. Conf. Exhibit. Electr. Distrib. (CIRED)*, Stockholm, Sweden, 2013, pp. 1–4.

[22] Y. Wang, D. Luo, X. Xiao, Y. Li, and F. Xu, "The problem of supraharmonic and its research status and trend," *Power Grid Technol.*, vol. 42, no. 02, pp. 353–365, 2018.

[23] D. G. Holmes and T. A. Lipo, "The modulation of single bridge inverter," in *Pulse Width Modulation for Power Converters: Principles and Practice*. Beijing, China: Posts and Telecom Press, 2003.

[24] J. Meyer, V. Khokhlov, M. Klatt, J. Blum, C. Waniek, T. Wohlfahrt, and J. Myrzik, "Overview and classification of interferences in the frequency range 2–150 kHz (supraharmonics)," in *Proc. Int. Symp. Power Electron., Electr. Drives, Autom. Motion (SPEEDAM)*, Amalfi, Duchy of Amalfi, Jun. 2018, pp. 165–170.

YINGXIN WANG was born in Zibo, Shandong, China, in 1995. She received the B.S. degree from Northeast Electric Power University. She is currently pursuing the Ph.D. degree with North China Electric Power University. Her research interest includes power quality and its control.

YONGHAI XU (Member, IEEE) was born in Xinye, Henan, China, in 1966. He received the B.S. degree from Tsinghua University, in 1989, the M.S. degree from North China Electric Power University (NCEPU), in 1992, and the Ph.D. degree from the Harbin Institute of Technology, in 2002.

He is currently a Professor with the School of Electrical and Electronic Engineering, North China Electric Power University. His research interests include power quality analysis and control, and new energy power systems.

SHUN TAO (Member, IEEE) was born in China, in November, 1972. She received the M.S. and Ph.D. degrees from North China Electric Power University (NCEPU) in 2005 and 2008, respectively. She had a Postdoctoral procedure at the Electrical Engineering Laboratory de Grenoble (G2Elab), Institute National Polytechnique de Grenoble (INPG), Grenoble, France, in 2010. She has been with the NCEPU, since 2008. Her research interest includes active distribution networks and its power-quality.

ABUBAKAR SIDDIQUE was born in Lodhran, Pakistan. He received the B.S. and M.S. degrees in electrical engineering from Islamia University Bahawalpur (IUB), Pakistan, in 2011 and 2013, respectively, and the Ph.D. degree from North China Electric Power University (NCEPU) Beijing, China, in 2019.

He is currently working as an Assistant Professor with the Department of Electrical Engineering, Khwaja Fareed University of Engineering and Information Technology (KFUEIT), Rahim Yar Khan, Pakistan. He has also worked at Islamia University Bahawalpur Pakistan. His research interests include power flow control, power electronics, and power system stability.

XU DONG was born in Taian, Shandong, China, in 1997. He received the B.S. degree in electrical engineering and automation from the Shandong University of Technology. He is currently pursuing the M.S. degree with North China Electric Power University. His research interest includes power quality and its control.